ISSN 1392 - 1207. MECHANIKA. 2011. 17(5): 540-544

Finite element analysis about stator of opposed biconinal cone screw high-pressure seawater hydraulic pump

Xinhua Wang, Xiuxia Cao, Gang Zheng, Shuwen Sun, Zhijie Li
College of Mechanical Engineering and Applied Electronics Technology, Beijing University of Technology, Beijing, China, E-mail: wangxinhua@bjut.edu.cn

crossref http://dx.doi.org/10.5755/j01.mech.17.5.733

1. Introduction

Modern marine equipment technology, which is for the marine environment and the integration of the current number of general technology, is an international cutting-edge technology. Sea water hydraulic technology compatible with the marine environment becomes a common technique which adapts to marine development and the development of modern marine equipment technology [1-4]. Sea water pump is the core power of the sea water hydraulic technology and the heart of the sea water hydraulic system [5], therefore the large number of studies are carried out aiming at the water hydraulic pump. The study on the sea water hydraulic pump is mainly the piston type sea water hydraulic pump at present, the critical friction pairs of the piston type sea water hydraulic pump are more, and the structure is complex, and high demands on the friction and wear, lubrication and seal, corrosion and pollution control technology are proposed. In addition, whether the axial piston pump or vane pumps or gear pumps, the structure will inevitably lead to some entrap phenomenon, which causes flow pulsation and pressure fluctuation, thus affecting the performance of the pump. Therefore, a new type opposed biconical cone screw high-pressure seawater hydraulic pump is designed in order to meet the requirements of modern marine equipment, particularly the requirements of equipment for deep diving operations.

The rubber bush of the stator is not only the damageable parts of the new pump, and the combining status between the stator and rotor has a significant impact on the performance of the new type pump, so the related research on the above problems are carried out and the deformation and stress of the bush and shell with the bush's inner cavity under the load are analyzed.

2. The structure and working principle of the opposed biconical cone screw high-pressure seawater hydraulic pump

The structure of the novel pump is shown in Fig. 1. The new type pump is mainly constituted by the a pair of cone screws (rotor), flexible wear-resistant bush (stator) which is equal thickness, pump body, left and right end cover, bearing, universal joint coupling, transmission shaft and seal, etc. Among them, the cone screw and flexible wear-resistant bush intermeshing in space, of which the cone screw and bush side composed, is two key core components of the novel pump. The cone screw do fixed-point movement, by the motor, transmission shaft through the universal joint coupling to drive to meet the requirements of fixed-point movement; the bush is fixed.

The external helicoids of the cone screw and the internal helicoids of the bush form a series of seal cavities, and the seal cavities go over the discharge end by spiral with the rotation of the cone screw. When the cone screw is rotating, the first cavity volume of the cone screw and bush side near the suction end increases gradually, and local vacuum is formed in the suction end, and the liquid is inhaled; meanwhile the last cavity near the discharge end disappears gradually and the liquid is squeezed out completely; with the continuous formation and lapse and disappearance of the seal cavity, the liquid is pushed from the suction end to the discharge end, and the pressure increases continuously, thus the entrap phenomenon of the existing hydraulic pump on the structure is thoroughly eliminated, so the flow change very uniformly. Because of the biconical opposition structure of the novel pump, the pump force balance in the axial direction, which eliminates the eccentric wear and leakage and other defects of the traditional. Positive displacement pump due to the power imbalance; meanwhile, the liquid in the seal cavity between the cone screw and bush can make the rotor in the bush generate dynamic and static back and center position, which will reduce the wear between the cone screw and bush and improve the running stability of the rotor about the novel pump. Besides, some initial interference value is designed between the cone screw and the bush in order to achieve a good seal, and reduce the internal leakage of the pump, and improve the volumetric efficiency of the pump; the friction side number of the new pump is much less than the number of the existing piston, and the new pump don't have any assignment device, so the structure of the novel pump is simple and the service life is long.

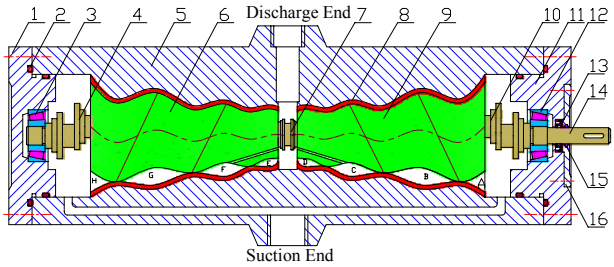

Fig. 1 The structure diagram of opposed biconical cone screw high-pressure seawater hydraulic pump: *1, 11* - big end cover; *2* - O-shape sealing ring; *3, 12* - bearing; *4, 7, 10* - universal joint; *5* - shell; *6, 9* - cone screw; *8* - flexible wear bush; *13* - FB-type rotation axis lip shape seal ring; *14* - rotary shaft; *15* - felt seal ring; *16* - small end cover

3. Contact finite element equation of the shell and bush

The problem is studied in the global three-

dimensional Cartesian coordinate system X, Y, Z. At the contact surface, however, the local Cartesian coordinate system $\bar{x}, \bar{y}, \bar{z}$ is defined in the following way. The coordinates systems is fixed to the shell. The $\bar{x}\bar{y}$-plane is a tangential plane and $\bar{z}$ is defined by an inward normal vector from the bush to the shell at the contact point studied.

3.1. The contact conditions and incremental stiffness equation of the contact boundary about the shell and bush

For $\{\Delta\bar{u}^{(a)}\}$, $\{\Delta\bar{u}^{(b)}\}$, $\{\Delta\bar{r}^{(a)}\}$ and $\{\Delta\bar{r}^{(b)}\}$ denote respectively the contact displacement incremental and contact force incremental of the two nodes *a* and *b* about the shell and bush at the local coordinate, so the boundary incremental form [6] of shell and bush with the adhesive contact condition is

$$\begin{array}{l} \Delta\bar{r}_i^{(a)} = -\Delta\bar{r}_i^{(b)} = \Delta\bar{r}_i \\ \Delta\bar{u}_i^{(a)} - \Delta\bar{u}_i^{(b)} + \bar{\delta}_i = 0 \end{array} \quad (i = x, y, z) \tag{1}$$

where $\bar{\delta}_i$ is the initial relative displacement, which is zero except for the initial state .

The matrix equation of the contact nodes pair *a* and *b* about the shell and bush with the adhesive contact condition are

$$\begin{bmatrix} [0] & [0] & -[I] \\ [0] & [0] & [I] \\ -[I] & [I] & [0] \end{bmatrix} \begin{Bmatrix} \{\Delta\bar{u}^{a}\} \\ \{\Delta\bar{u}^{b}\} \\ \{\Delta\bar{r}\} \end{Bmatrix} = \begin{Bmatrix} -\{\Delta\bar{r}^{(a)}\} \\ -\{\Delta\bar{r}^{(b)}\} \\ \{\bar{\delta}\} \end{Bmatrix} \tag{2}$$

where

$$\{\bar{\delta}\} = \left[\bar{\delta}_x, \ \bar{\delta}_y, \ \bar{\delta}_z\right]^T, \ \{\Delta\bar{u}^{i}\} = \left[\Delta\bar{u}_x^{(i)}, \ \Delta\bar{u}_y^{(i)}, \ \Delta\bar{u}_y^{(i)}\right]^T,$$

$$\{\Delta\bar{r}^{i}\} = \left[\Delta\bar{r}_x^{(i)}, \ \Delta\bar{r}_y^{(i)}, \ \Delta\bar{r}_y^{(i)}\right]^T \ (i = a, b)$$

When the contact nodes *a* and *b* are considered as a element, the Eq. 2 will be the increment stiffness equation of the element. The increment stiffness equation of the contact boundary is the combination of all the contact elements stiffness equations on the boundary. When there are *N* contact nodes(pairs) on the contact boundary, the increment equation of the contact boundary is

$$\begin{bmatrix} [0] & [0] & -N[I] \\ [0] & [0] & N[I] \\ -N[I] & N[I] & [0] \end{bmatrix} \begin{Bmatrix} \{\Delta\bar{U}^{a}\} \\ \{\Delta\bar{U}^{b}\} \\ \{\Delta\bar{R}^{N}\} \end{Bmatrix} = \begin{Bmatrix} -\{\Delta\bar{R}^{(a)}\} \\ -\{\Delta\bar{R}^{(b)}\} \\ \{\bar{\Delta}\} \end{Bmatrix} \tag{3}$$

where $\{\bar{\Delta}\} = \sum_i^N \{\bar{\delta}^{i}\}$, $\{\Delta\bar{U}\}$ and $\{\Delta\bar{R}\}$ are the contact displacement increment and contact force increment respectively.

3.2. Increment finite element equation of shell and bush with the adhesive contact condition

By the principle of virtual work, the increment finite element equation [7] of the shell and bush about the contact structure at the total coordinate is

$$\left[K^{(I)}\right]\left\{\Delta U^{(I)}\right\} = \left\{\Delta P^{(I)}\right\} + \left\{\Delta R^{(I)}\right\} \tag{4}$$

where $\left[K^{(I)}\right]$ is the total stiffness matrix of the shell or bush, $\left\{\Delta U^{(I)}\right\}$, $\left\{\Delta P^{(I)}\right\}$ and $\left\{\Delta R^{(I)}\right\}$ are the increment vector of the corresponding nodal displacement, load and contact force respectively.

The block of the Eq. (4) is by the contact boundy nodes and noncontact boundy nodes, and the α and β are the noncontact area and contact area respectively, so the Eq. (4) will be transformed into

$$\begin{bmatrix} \begin{bmatrix} K_{\alpha\alpha}^{(I)} \\ K_{\beta\alpha}^{(I)} \end{bmatrix} & \begin{bmatrix} K_{\alpha\beta}^{(I)} \\ K_{\beta\beta}^{(I)} \end{bmatrix} \end{bmatrix} \begin{Bmatrix} \{\Delta U_{\alpha}^{(I)}\} \\ \{\Delta U_{\beta}^{(I)}\} \end{Bmatrix} = \begin{Bmatrix} \{\Delta P_{a}^{(I)}\} \\ \{\Delta P_{\beta}^{(I)}\} \end{Bmatrix} + \begin{Bmatrix} \{0\} \\ \{\Delta R_{\beta}\} \end{Bmatrix} \tag{5}$$

By the coordinate change and combination with the Eq. (3), the increment finite element equation of the shell and bush with the adhesive contact condition is

$$\begin{bmatrix} \begin{bmatrix} K_{\alpha\alpha}^{(A)} \\ \overline{K}_{\beta\alpha}^{(A)} \end{bmatrix} & \begin{bmatrix} \overline{K}_{\alpha\beta}^{(A)} \\ \overline{K}_{\beta\beta}^{(A)} \end{bmatrix} & [0] & [0] & [0] \\ [0] & [0] & \begin{bmatrix} K_{\alpha\alpha}^{(B)} \\ \overline{K}_{\beta\alpha}^{(B)} \end{bmatrix} & \begin{bmatrix} \overline{K}_{\alpha\beta}^{(B)} \\ \overline{K}_{\beta\beta}^{(B)} \end{bmatrix} & [0] \\ [0] & -N[I] & [0] & N[I] & [0] \end{bmatrix} \begin{Bmatrix} \{\Delta U_{\alpha}^{(A)}\} \\ \{\Delta\overline{U}_{\beta}^{(A)}\} \\ \{\Delta U_{\alpha}^{(B)}\} \\ \{\Delta\overline{U}_{\beta}^{(B)}\} \\ \{\Delta\overline{R}^{(N)}\} \end{Bmatrix} =$$

$$= \begin{Bmatrix} \{\Delta P_{\alpha}^{(A)}\} \\ \{\Delta\overline{P}_{\beta}^{(A)}\} \\ \{\Delta P_{\alpha}^{(B)}\} \\ \{\Delta\overline{P}_{\beta}^{(B)}\} \\ \{\Delta\} \end{Bmatrix} \tag{6}$$

where $\left\{\Delta\overline{U}_{\beta}^{(I)}\right\}$, $\left\{\Delta\overline{P}_{\beta}^{(I)}\right\}$ and $\left\{\Delta\overline{R}_{\beta}^{(I)}\right\}$ are the corresponding amount at the local coordinate, $\left[\overline{K}_{\alpha\beta}^{(I)}\right]$, $\left[\overline{K}_{\beta\alpha}^{(I)}\right]$ and $\left[\overline{K}_{\beta\beta}^{(I)}\right]$ are the amount of the local coordinate into which the total coordinate changes.

4. The finite element analysis of the space model and plane model about the shell and bush

4.1. The finite element analysis of the space model

The internal surface of the shell and the internal and external surface of the bush about the new pump are both the double line helicoids, the internal surface of the bush is shown as the Figs. 2 and 3.

The parameters of the bush are set as follow: half

cone angle of the static instantaneous axis trajectory cone $\eta = 28'$, half cone angle of the generated cone $\theta = 1°32'$, the stator's pitch $T = 50$ mm, the distance from the end of bush to the pole: large end $\rho_1 = 390$ mm, small end $\rho_2 = 290$ mm, the thickness of the bush at the large end is 5.3 mm, and the thickness of the bush at each section is proportional to the distance from the each section to the pole, then the solid model of the bush is established.

Fig. 2 The first/second conjugate surface

In order to improve computational efficiency, the distance from the small end to the pole (the origin of coordinate) is set as 350 mm, and the distance from the large end to the pole is set as 390 mm, then the finite element analysis model of the shell and bush is established by the ANSYS. When the finite element model of the shell and bush is analyzed, the material model of the shell is linear elastic, and the elastic modulus is 210 GPa, and the Poisson's ratio is 0.3; the Mooney-Rivlin model of the rubber is used to simulate the constitutive relation of the rubber material about the bush, and the constitutive relation of the rubber material about the bush is set as linear elastic, and the elastic modulus is 4 MPa, and the Poisson's ratio is 0.499 [8].

About the novel pump, the two ends of the shell are fixed with the end cover by the bolt, so displacement constrains of all directions are applied on the two ends and the external surface of the shell. When the uniform pressure is imposed on the internal surface of the bush, the calculation result of the space deformation about the shell and bush after the pressure applied is shown as Fig. 3, and the calculation results of the space stress about the shell and bush are shown as Fig. 4.

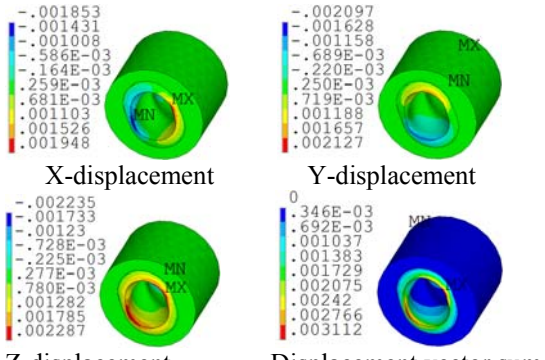

Fig. 3 The space displacement of the stator

Under the above load and constraints conditions, what can be seen from the Fig. 3 is that: the maximum deformation of the X direction is at the second conjugate surface of the bush's intracavity, and the value is 1.948 mm; the maximum deformation of the Y direction is at the first conjugate surface of the bush's intracavity, but near the second conjugate surface, and the value is 2.287 mm; the maximum deformation of the Z direction is at the contact department of the first conjugate surface and the second conjugate surface about the bush's intracavity, and the value is 2.287 mm; the maximun displacement vector of the bush is at the contact deparment of the first conjugate surface and the second conjugate surface about the bush's intracavity, and the value is 3.112 mm, the displacement vector of the shell is zero [9, 10].

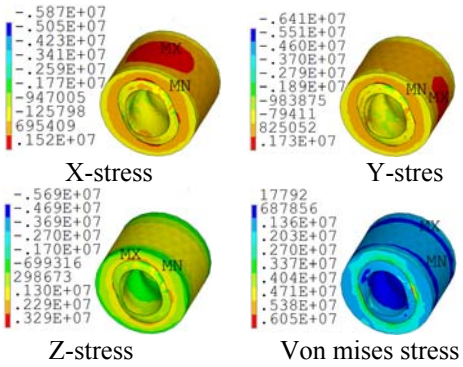

Fig. 4 The space stress of the shell and bush

Under the above load and constraints conditions, what can be seen from the Fig. 4 is that: the maximum stress of the X and Y direction about the shell is at the first conjugate surface of the shell's middle, and the value is respectively 1.52 and 1.73 MPa; the maximum stress of the Z direction is at the first conjugate surface of the shell's end, the value is 3.29 MPa; at the Von Mises stress distribution diagram of the shell, the maximum stress is at the end of the shell. At the X, Y, Z and Von Mises stress distribution diagram of the bush, the maximum stress all are at the end of the bush, and the von stress gradually decreases from the end of the bush to the middle of the bush.

4.2. The plane model analysis of the shell and bush

In order to compare the similarities and differences of the displacement and stress about the plane and space model when the internal intracavity of the bush is applied the uniform pressure, the plane model with 390 mm from the coordinate origin of the new type pump is established in ANSYS.

The displacement constrains of X and Y direction are applied on the outer cylinder of the shell, and the uniform pressure is applied on the inner circle of the bush, then the calculation results of the plane deformation and stress about the shell and bush after the pressure applied is shown as the Fig. 5 and 6.

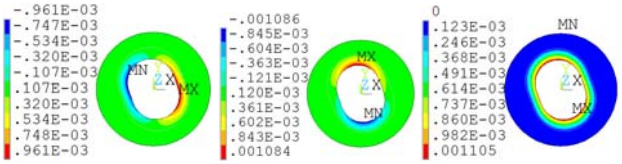

Fig. 5 The plane deformation of the shell and bush

Under the above load and constraints conditions, what can be seen from the Fig. 5 is that: the maximum deformation of the X direction is at the contact department of the first conjugate surface and the second conjugate surface about the bush's intracavity, and the value is 0.961mm; the maximum deformation of the Y direction is at first conjugate surface of the bush's intracavity, and the value is 1.084 mm; the displacement vector of the shell is zero, and

the maximum displacement vector of the bush is at the middle of the first conjugate surface about the bush's intracavity, and the value is 1.105 mm.

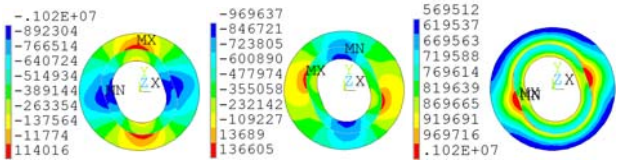

Fig. 6 The plane stress of the shell and bush

Under the above load and constraints conditions, what can be seen from the Fig. 6 is that: the maximum stress of the X direction is at the second conjugate surface of the bush and shell, the value is 1.02 MPa; the maximum stress of the Y direction is at the first conjugate surface of the bush's intracavity, and the value is 0.9696 MPa; at the Von Mises stress distribution diagram, the maximum stress is at the contact department which is at middle of the second conjugate surface about the shell the of the shell and bush, and the value is 1.02 MPa; the stress distributions of the shell and bush are both law which the stress decreases from the inside to outside.

5. Conclusion

Trough the finite element analysis of the plane model and space model with the stator about the new pump, the following conclusions can be drawn:

1. At the space model of the stator, the maximum deformation of the X direction is at the second conjugate surface of the bush's intracavity; the maximum deformation of the Y direction is at the first conjugate surface of the bush's intracavity, but near the second conjugate surface; the large deformation damage is easily caused at the contact position of the first conjugate surface and the second conjugate surface. At the plane model of the stator, the maximum deformation of the X direction is at the contact department of the first conjugate surface and the second conjugate surface about the bush's intracavity; the maximum deformation of the Y direction is at first conjugate surface of the bush's intracavity.

2. At the space model of the stator, the maximum stress of the X and Y direction is at the contact position of the first conjugate surface and the second conjugate surface about the bush's external surface; At the plane model of the stator, the maximum stress of the X direction is at the second conjugate surface of the bush's external surface; the maximum stress of the Y direction is at the first conjugate surface of the bush's internal surface.

3. The maximum deformation and stress on all direction of the plane model and space model about the shell and bush of the novel high-pressure seawater hydraulic pump have much difference, so the plane model of the shell and bush about the new pump can't replace the space model on the finite element analysis.

References

1. **Tao Aihua; Yang Shudong; Yu Zuyao; Li Zhuangyun.** 2003. Simulation of the seawater hydraulic powered underwater operation tools system, Machine Tool and Hydraulics, 2: 189-191.
2. **Nie Songlin; Liu Yinshui; Yu Zuyao; Li Zhuangyun,** 2004. Development of an underwater tool system driven by seawater hydraulics, The Ocean Engineering, Vol. 22: 87-91.
3. **Yang Shudong; Li Anyua; Tao Aihua**, 2007. Development of a high pressure seawater hydraulic pump lubricated with seawater, Hydraulic and Pneumatic 10: 15-17.
4. **Cao Xuepeng; Wang Xiaojuan; Deng Bin; Ke Jian**. 2010. The development status and key techniques of deep-sea hydraulic power source, Marine Science Bulletin, vol 29(4): 466-471.
5. **Zhao Jisong; Yang Shudong.** 2005. Pilot study about the contaminant sensitivity of seawater hydraulic pumps, Hydraulic and Pneumatic, Vol. 4: 68-70.
6. **Okamoto, N.; Nakazawa, M.** 1979. Finite element in increment contact analysis with various frictional conditions, Int. J. MUM. Meth. Engng. 14: 337-357.
7. **Yang Xianqi; Li Xiaoling**. The Theory and Technology and Application of Modern Finite Element, edited by Beihang University Press.
8. **Wei Yintao; Yang Tingqingp; Du Xingwen**. 1999. On the large deformation rubber-like materials: constitutive law and finite element method, Acta Mechanica Solida Sinica,vol.20(4): 281-289.
9. **Yeoh, O.H**. 1993. Some forms of the stain energy function for rubber, Rubber Chemistry and Technology 66: 754-771.
10. **Petkevičius, K.; Volkovas, V.** 2011. Monitoring and identification of structural damages, Mechanika 17(3): 246-250.

Xinhua Wang, Xiuxia Cao, Gang Zheng, Shuwen Sun, Zhijie Li

HIDRAULINIO SIURBLIO STATORIAUS SU DVIGUBO KŪGIO KŪGINIU SRIEGIU PASIPRIEŠINIMO DIDELIAM JŪROS VANDENS SLĖGIUI ANALIZĖ BAIGTINIŲ ELEMENTŲ METODU

R e z i u m ė

Statoriaus guminė įvorė yra ne tiktai pažeidžiamiausia didelio slėgio hidraulinio siurblio su dvigubo kūgio kūginiu sriegiu detalė, bet ir jungia statorių ir rotorių, todėl turi didelę reikšmę šio naujo tipo siurblio darbui. Šis tyrimas ir skirtas pažeidžiamumo priežasčiai nustatyti. Sudarytos korpuso ir įvorės kontaktinių baigtinių elementų lygtys, baigtinių elementų metodu analizuojant statoriaus deformacijas ir įtempius, diskutuojama, ar plokščiasis modelis gali pakeisti erdvinį. Analizė parodė, kad deformacija ir įtempiai, nustatyti naudojant statoriaus plokščiąjį ir erdvinį modelius, gerokai skiriasi, todėl, atliekant tyrimą baigtinių elementų metodu, plokščiasis modelis negali pakeisti erdvinio.

Xinhua Wang, Xiuxia Cao, Gang Zheng, Shuwen Sun, Zhijie Li

FINITE ELEMENT ANALYSIS ABOUT STATOR OF OPPOSED BICONINAL CONE SCREW HIGH-PRESSURE SEAWATER HYDRAULIC PUMP

S u m m a r y

The rubber bush of the stator is not only the damageable parts of the opposed biconinal cone screw high-pressure seawater hydraulic pump, and the combining status between the stator and rotor has a significant impact on the performance of the new type pump, so the related research on above problems are carried out. The contact finite element equation of the shell and bush is established and the deformation and stress of the stator's space and plane's model under the force state are compared and analyzed with the finite element method, and discuss whether the plane model could replace the space model on the finite element analysis of the deformation and stress about the stator. The analysis shows that the deformation and stress of the stator's plane model and space model have much difference, so the plane model can't replace the space model on the research of the finite element analysis.

Received February 25, 2011
Accepted September 09, 2011